Acta
Materia
Medica

Research Article

Inhalable ciprofloxacin/polymyxin B dry powders in respiratory infection therapy

Graphical abstract

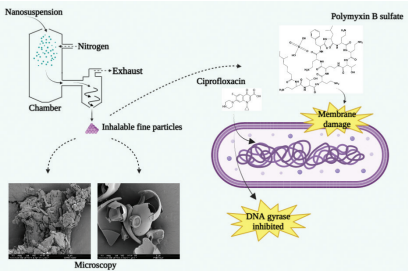

Highlights

- Spray-dried inhalable dry powders containing ciprofloxacin and polymyxin B sulfate exhibited good aerosol performance with the fine particle fractions above 50%.
- The presence of polymyxin B sulfate enhances the aerosol performances of the spray-dried dry powder formulations.
- Spray-dried inhalable dry powders containing ciprofloxacin and polymyxin B sulfate exhibited antimicrobial effects against *Pseudomonas aeruginosa* strain PAO1.

Authors

Zhengqi Xu, Hriday Bera, Hengzhuang Wang, Junwei Wang, Dongmei Cun, Yu Feng and Mingshi Yang

Correspondence

marshimaro_star@sina.com (Y. Feng);
mingshi.yang@sund.ku.dk (M. Yang)

In brief

A novel spray-dried inhalable dry powders with improved aerosol performance and antimicrobial effects was developed to exert antimicrobial combination effect of ciprofloxacin and polymyxin B sulfate for the treatment of respiratory infection.

https://doi.org/10.15212/AMM-2022-0050

Acta Materia Medica

Research Article

Inhalable ciprofloxacin/polymyxin B dry powders in respiratory infection therapy

Zhengqi Xu[a,1], Hriday Bera[b,c,1], Hengzhuang Wang[d,e], Junwei Wang[a], Dongmei Cun[b], Yu Feng[b,*] and Mingshi Yang[a,b,*]

[a]Department of Pharmacy, University of Copenhagen, Universitetsparken 2, DK-2100 Copenhagen, Denmark
[b]Wuya College of Innovation, Shenyang Pharmaceutical University, Wenhua Road No. 103, 110016 Shenyang, China
[c]Dr. B.C. Roy College of Pharmacy and Allied Health Sciences, Durgapur 713206, India
[d]Department of Clinical Microbiology, Copenhagen University Hospital, Rigshospitalet, Henrik Harpestrengsvej 4A, DK-2100 Copenhagen, Denmark
[e]Department of Immunology and Microbiology, University of Copenhagen, Blegdamsvej 3B, DK-2200 Copenhagen, Denmark

[1]Contributed equally.
***Correspondence:** marshimaro_star@sina.com (Y. Feng); mingshi.yang@sund.ku.dk (M. Yang)

Received: 26 December 2022; Revised: 29 March 2023; Accepted: 3 April 2023

Published online: 29 April 2023

DOI 10.15212/AMM-2022-0050

ABSTRACT

The current study focused on the formulation, physicochemical characterization, and antibacterial susceptibility testing of inhalable spray dried powders containing ciprofloxacin (CIP) and polymyxin B sulfate (PMB). CIP nanosuspensions with an average particle diameter of 435.9 ± 9.3 nm were initially obtained using the wet-milling protocol and subsequently co-spray dried with PMB solutions to yield inhalable dry powders. The Powder X-Ray Diffraction (P-XRD) results showed that the wet-milled CIP nanoparticles were in a 4.8 hydrate state, which were transformed to 3.7 hydrates and amorphous materials after co-spray drying. The PMB remained in an amorphous state in the dry powders. Differential Scanning Calorimetry (DSC) analyses revealed that the glass transition temperatures (T_gs) of the co–spray dried formulations were higher than the T_g of CIP, but lower than the T_g of PMB. Fourier Transform Infrared Spectrometer (FTIR) studies suggested the existence of π - π interactions between CIP and PMB in the co-spray dried powders. These powders also retained antimicrobial effects against *Pseudomonas aeruginosa* strain PAO1. In addition, the spray-dried powder formulations exhibited satisfactory solid-state stability and aerodynamic characteristics when stored under 3% relative humidity and 20 ± 5 °C for 4 months. Overall, the newly developed inhalable CIP/PMB dry powders are a promising therapeutic strategy for respiratory tract infections.

Keywords: Inhalable dry powders, Nanosuspensions, Co-spray drying, Solid state characteristics, Aerodynamic properties, Antibiotic susceptibility

1. INTRODUCTION

Respiratory tract infections (RTIs), especially infections involving the lower respiratory tract, are the major cause of morbidity and mortality worldwide [1]. Aggravation of such illness states often leads to the production of sputum and purulence, and shortness of breath, which negatively affect a patient's quality of life [2]. According to recent research [3], greater than 2 million people died due to RTIs in 195 countries in 2016, which ranked sixth among deaths in all age groups. Thus, the treatment of RTIs and control of related mortality are an unmet need.

Numerous antibiotics are commonly prescribed to treat RTIs which effectively eliminate bacteria, including *Pseudomonas aeruginosa*, *Haemophilus influenzae*, *Moraxella catharralis*, and *Streptococcus pneumoniae*. Antibiotic therapy can reduce the bacterial load and prevent the acquisition of new bacterial strains; however, the conventional oral delivery of antibiotics might introduce drug resistance owing to repeated usage, high dose, and abuse of broad-spectrum drug activity [4], thus reducing the treatment efficacy of antimicrobial therapy. To avoid drug resistance and effectively treat RTIs, the delivery of antibiotics via the

pulmonary route has long been adopted as a potential strategy. Compared to oral administration, antibiotic delivery via the pulmonary route might easily achieve a higher local drug concentration with lower systemic exposure [5]. Consequently, this approach could lead to lower systemic toxicity, decreased drug resistance, and enhanced therapeutic efficacy. In this context, combination therapy of antibacterial agents, such as tobramycin/colistin and tobramycin/clarithromycin, has been used to successfully eradicate RTIs. Specifically, inhaled tobramycin/colistin is well-tolerated in patients with cystic fibrosis, and results in an average decrease in *P. aeruginosa* by 2.52 ± 2.5 $\log_{10}$ cfu/ml of sputum. Pioneering studies have demonstrated a better therapeutic outcome of combination therapy to combat bacterial infections relative to monotherapy [6]. It has also been shown that co-administration of antibiotics via the pulmonary route into solid states dramatically improves drug performance [7-10]. For example, aerosolization and physical stability of ciprofloxacin (CIP)/colistin spray dried powders were notably enhanced due to powder surface modification and intermolecular interactions [7].

In an analogous approach, CIP, a first-line drug for RTIs with a high propensity to developing resistance, can be combined with polymyxin B sulfate (PMB) for delivery as inhalable dry powders. It is noteworthy that PMB is a cornerstone antibiotic used in the treatment of multidrug-resistant bacteria that acts by destabilizing the outer membrane of Gram-negative bacteria, which also facilitates the entry of other antibiotics into bacterial cells [11, 12]. Our recent study showed that the combination of CIP and PMB exerts a synergistic effect against multidrug-resistant bacteria [13]; however, considerable work remains to develop this drug pair into inhaled formulations. In this study we investigated the potential of formulating this drug combination into dry powders for inhalation. Dry powder formulations containing CIP and PMB at different ratios were prepared. The aerodynamic performance before and after storage were evaluated. In addition, the antimicrobial efficacy of the drug combinations was investigated.

2. MATERIALS AND METHODS

2.1 Materials

CIP anhydrate (zwitterionic form) and PMB were obtained from Nanjing Sunlidabio Pharmaceutics (Nanjing, Jiangsu, China). Tween 20 and glass beads (0.5 and 1.0 mm in diameter) were purchased from Sigma-Aldrich (St. Louis, MO, USA). *P. aeruginosa* strain PAO1 was cultured in the Department of Clinical Microbiology at the University Hospital of Copenhagen (Copenhagen, Denmark). Mueller-Hinton agar plates were purchased from the Denmark State Serum Institute (Copenhagen, Denmark). All other chemicals were of analytical grade.

2.2 Preparation of CIP nanosuspensions and the particle size analyses

The CIP nanosuspensions were prepared using the wet milling method based on previous reports [14, 15]. Specifically, an accurately measured quantity of CIP (300 or 600 mg) was suspended in de-ionized water (28-40 mL) contained in a 100-mL glass container with a lid. Glass beads (i.e., a mixture of 0.5- and 1.0-mm glass beads at a 1:1 ratio [w/w]) were added to these suspensions to make a 2:1 ratio between the glass beads and water. The suspensions were then agitated at a maximum stirring speed on a magnetic stirrer (IKA® RH basic; IKA®-Werke GmbH & Co. KG, Staufen, Germany) at room temperature for 24 h to produce CIP nanosuspensions.

The mean hydrodynamic size (z – average) and polydispersity index (PDI) of the CIP nanoparticles were measured using Zetasizer Nano ZS (Malvern Panalytical, Malvern, UK) with 173° optics for detection at 25 °C. The size distribution of nanoparticles is described as the span, which was calculated according to following expression:

$$\text{Span}=\frac{d_{0.9}-d_{0.1}}{d_{0.5}},$$

where $d_{0.1}$ and $d_{0.9}$ refer to particle diameters at 10% and 90% of the cumulative distribution, respectively.

2.3 Preparation of CIP/PMB co-spray dried powders

Five different kinds of CIP/PMB co-spray dried powders were generated following previously published protocols. Briefly, variable concentrations of PMB aqueous dispersions were mixed with diluted CIP nanosuspensions at room temperature by magnetic stirring (100 rpm) for 10 min. The final solid content of different formulations was fixed at 20 mg/mL. The mixtures were then spray-dried by a Büchi B-290 spray dryer (Büchi Labortechnik AG, Postfach, Switzerland) using a two-fluid nozzle (Büchi Labortechnik AG, Flawil, Switzerland) and a dehumidifier (Büchi Labortechnik AG, Flawil, Switzerland). The nozzle hole diameter of the Buchi B-290 spray dryer was 0.7 μm. Several spray drying parameters, including a feed rate of 2.4 mL/min, an inlet temperature of 120 °C, an outlet temperature between 70 °C and 75 °C, a drying air flow rate of 37.5 m^3/h, and an atomization air flow rate of 601 L/h were fixed. The percent yield of each spray-dried powders was calculated based on the following relationship:

> yield (%) = mass of drug powder collected after spray-drying (mg)/mass of drugs in the feed solution (mg) × 100.

2.4 Drug content

To evaluate the drug content in spray-dried powders, the samples were dissolved in 30 mM sodium sulfate solution and the mass content of CIP and PMB were quantified using the HPLC method.

2.5 Moisture content

The moisture content of spray-dried powders was detected using a Discovery Thermogravimetric Analyzer [TGA] (TA Instruments, New Castle, Delaware, USA). The weight loss in the heating process (heating rate, 10°C/min) within 25-140°C was considered the moisture content of the formulations.

2.6 Scanning electron microscopy (SEM) analyses

The nanosuspensions were ultracentrifuged (Optima™ Max-XP Ultracentrifuge; Beckman Coulter, Brea, CA, USA) and the pellets were collected. Images of the dried pellets were acquired on a SEM (Hitachi High – Tech Hitachi, Santa Clara, CA, USA) at 5000× magnification.

The CIP/PMB co-spray dried powders were sputter-coated with gold using a Leica EM ACE 200 (Vienna, Austria). The images were captured using an FEI Quanta 3D FEG (FEI, Hillsboro, OR, USA) at 20,000× magnification.

2.7 XRD studies

Sample diffractograms were recorded within 2θ of 5-35° on a X'Pert PRO X-ray diffractometer (PANalytical, Almelo, The Netherlands) fitted with a CuKα radiation source (k = 1.54060 Å). The operating current and voltage were set at 40 mA and 45 kV, respectively.

2.8 DSC analyses

Raw drugs and spray-dried powders were sealed on a Tzero aluminum pan and heated on a Discovery differential scanning calorimeter [DSC] (TA Instruments) within a wide temperature range (5°C-29°C) at a linear heating rate of 2°C/min. The heat flow sample data were analyzed using Trios software (TA Instruments).

2.9 FT-IR analyses

Pristine drugs and spray-dried powders were scanned under Fourier-transform infrared spectroscopy (Nicolet 380 FT-IR spectrometer; Thermo Scientific, Waltham, MA, USA) within the wavenumber range of 4000-400 cm^{-1}.

2.10 Aerodynamic properties

The aerodynamic characteristics of different spray-dried powders were assessed using a Next Generation Impactor [NGI] (Copley Scientific, Nottingham, UK). All NGI stages, including the micro-orifice collector (MOC), were coated with 4 mL of 30 mM sodium sulfate (pH 2.5, adjusted with phosphoric acid) and Tween 20 mixture (95:5 [v/v]) to avoid bounce of the powders during deposition. Approximately 10 mg of powders were loaded in a hydroxypropyl methylcellulose capsule (size 3; Capsugel, West Ryde, Australia) and actuated using an ICOcap® dry powder inhaler device (Iconovo, Lund, Sweden). The aerodynamic performance parameters, such as the emitted dose fraction (ED, %), recovered dose (RD), fine particle fraction of the total dose (FPF_{total}, %), and the median mass aerodynamic diameter (MMAD), were investigated at a flow rate of 100 L/min for 2.4 s.

To examine the influence of drug doses in the capsules on the aerodynamic properties, approximately 10 mg, 20 mg, and 30 mg of powders were loaded in a hydroxypropyl methylcellulose capsule, actuated by an ICOcap® dry powder inhaler device, and the aerodynamic behavior was compared.

2.11 Antibacterial susceptibility test

The spray-dried formulations (F1-F5) were evaluated for susceptibility on PAO1 using the Kirby-Bauer disk diffusion method [16]. The PAO1, especially the *P. aeruginosa* strain PAO1 inoculum with 10^8 colony-forming units (CFU)/mL (EUCAST, 0.5 MacFarland standard) was inoculated on Muller-Hinton agar plates using a sterile swab [17, 18]. The plates were inoculated by thrice-streaking the swab over the agar surface, rotated approximately 60°, and dried. Then, cellulose disks were placed onto the surface of the agar with forceps and 20 µL of diluted (250 µg/mL) antimicrobial formulations (F1-F5) were transferred to the disks at 35°C ± 2°C. The diameters of inhibition zones were measured after 24 h.

2.12 Stability test

Different spray-dried powders (F1-F5) were stored under 2 different conditions, as follows: 60 ± 5 % relative humidity/20 ± 5 °C temperature (accelerated test condition); and 3 % relative humidity/20 ± 5 °C temperature. The different spray-dried powders were tested using an X-ray diffractometer and NGI after 1, 2, and 4 months of storage.

2.13 HPLC analyses of CIP and PMB

The concentrations of CIP and PMB in various samples were quantified using an Agilent 1260 infinity high-performance liquid chromatography (HPLC) system (Agilent, Santa Clara, CA, USA) equipped with an Agilent 1290 diode array detector. The samples were dissolved in 30 mM sodium sulfate solution (pH 2.5, adjusted with phosphoric acid), and 20 µL of solution was injected into an Ultremex™ C18 column (Column length 150 mm × internal diameter 4.6 mm, particle size 5 µm; Phenomenex, Torrance, CA, USA) at a flow rate of 1.0 ml/min. CIP and PMB were detected using an ultraviolet detector at 215 nm. The mobile phase was a mixture of 22 % (v/v) acetonitrile and 78 % sodium sulfate solution [v/v] (30 mM; pH 2.5, adjusted with phosphoric acid). The correlation curve for CIP was linear in the concentration range of 0.7 - 140 µg/mL ($r^2 > 0.999$) and the limit of quantification was 50 ng/mL. The correlation curve for PMB was linear in the range of 15 – 1800 µg/mL ($r^2 > 0.999$) and the limit of quantification was 8 µg/mL.

2.14 Statistical analysis

All experimental data are presented as mean values ± standard deviation (SD). Statistically significant

differences were assessed by one-way analysis of variance (ANOVA) or a t-test at a 0.05 significance level (SPSS Statistics; IBM, Armonk, NY, USA).

3. RESULTS AND DISCUSSION

3.1 Preparation of CIP nanosuspensions and the size distributions

In the current study specialized particle engineering technology (i.e., spray-drying) was used to generate inhalable CIP/PMB dry powders with improved physical and aerosolization stability. Various spray-dried small molecule drugs, such as CIP, can be transformed into an amorphous form and tend to crystalize upon storage, exhibiting poor aerosolization behaviour. The synergistic PMB, a high molecular weight polypeptide antibiotic, retains an amorphous state on storage and acts as a polymer-like matrix that minimizes mobility of CIP molecules, thus inhibiting the crystallization tendency for amorphous CIP, eventually, yielding an optimum aerosol performance of inhalable CIP/PMB dry powders. Prior to spray-drying, CIP nanosuspensions were generated via the wet milling protocol to minimize the CIP particle sizes and derive the most evenly distributed products. In this context, the effects of the two most important process parameters, including the CIP mass (mg) and milling medium volume (mL), on the sizes, PdI, and span values of the CIP nanoparticles were investigated (Table 1). Mono-dispersed particles were produced with a z-average of 435.9 ± 9.3 nm and a significantly lower PdI and span value ($p < 0.05$) under conditions in which the drug mass and volume of the milling medium were 40.0 mL and 600 mg, respectively. A high degree of milling between an abundance of drug molecules and milling medium might yield a narrow size distribution of CIP nanoparticles. Consequently, this condition was adopted as the most suitable condition to prepare CIP nanosuspensions.

Table 1 | Preparation parameters of CIP nanosuspensions and the size distributions.

Mass of CIP (mg)	Volume of milling medium (mL)	Z – Average (nm)	PdI	Span
300.0	28.0	454.7 ± 10.3	0.499 ± 0.087	1.9 ± 0.1
	32.0	414.3 ± 14.4	0.674 ± 0.121	1.4 ± 0.2
	36.0	423.5 ± 32.1	0.618 ± 0.055	1.5 ± 0.2
	40.0	956.8 ± 12.3	0.511 ± 0.023	1.2 ± 0.3
600.0	28.0	521.1 ± 40.2	0.551 ± 0.128	1.4 ± 0.1
	32.0	461.8 ± 9.7	0.677 ± 0.032	2.6 ± 0.1
	36.0	556.0 ± 55.9	0.617 ± 0.084	1.5 ± 0.3
	40.0	435.9 ± 9.3	0.202 ± 0.028	0.7 ± 0.1

3.2 Preparation of spray-dried powders

The resulting CIP nanosuspensions were mixed with PMB solutions in various proportions (Table 2) and co-spray-dried to afford dry powders (F1-F5) at an inlet temperature of 120 °C. The content of PMB in the spray-dried powders was slightly decreased compared to pristine PMB with a further increase in the inlet temperature (**Figure S1**). This feature can be accredited to the fact that the polypeptide PMB might be prone to degradation by heat, shear, dehydration, and interfacial stresses involved in spray-drying technology. The yield of the spray-dried powders increased as the PMB content increased (Table 2). Specifically, F1 exhibited the lowest yield (43.8 ± 3.7%), while F5 had the highest yield (64.1 ± 0.3%). The decrease in the formulation yield with an increase in the CIP content might be explained by high moisture content as determined by TGA analyses (Table 2) and hygroscopicity of spray-dried CIP. The powders containing a greater proportion of CIP became sticky and adhered to the inner wall of the spray drier. The CIP and PMB mass content in various formulations (F1-F5) was quantified using HPLC analyses (Table 2). The CIP mass content in F1 was 89.1% and the PMB mass content

Table 2 | Composition of the spray-dried powders and the yield, measured mass content of drugs, moisture content, and PAO1 growth inhibition zones.

Formulations	Concentration of CIP Nanosuspensions (mg/mL)	Concentration of PMB (mg/mL)	Yield (%)	Measured CIP mass content (%)	Measured PMB mass content (%)	Moisture content (%)	PAO1 growth inhibition zones (mm)
F1	20	0	43.8 ± 3.7	89.1 ± 0.6	-	14.5 ± 0.2	16
F2	16	4	57.3 ± 0.6	69.0 ± 0.2	20.8 ± 0.1	13.4 ± 0.1	15
F3	10	10	59.7 ± 0.5	38.7 ± 0.2	51.7 ± 0.3	11.2 ± 0.3	12
F4	4	16	60.3 ± 0.6	17.0 ± 0.3	73.4 ± 0.3	10.2 ± 0.2	11
F5	0	20	64.1 ± 0.3	-	92.1 ± 0.8	8.7 ± 0.1	10

Moisture content of CIP raw materials, 0.4.
Moisture content of PMB sulfate raw materials, 9.6.

Acta Materia Medica

in F5 was 92.1%. In addition, the measured CIP mass content in F2, F3, and F4 was significantly lower than the theoretical values, which could be associated with moisture content. Based on the TGA analyses results, the native CIP and PMB moisture content was 0.4% and 9.6%, respectively. Interestingly, the water content in F1 (14.5%) was greater than the water content in F5 (8.7%), and the water content was enhanced with an increase in the CIP content of the formulations (Table 2). This finding confirmed that the CIP molecules were in a hydrate state, resulting in a lower CIP mass content in various spray-dried powders than the theoretical values.

3.3 Morphology

The SEM images of native CIP and PMB, wet-milled CIP, and various spray-dried powders were compared (Figure 1). The pristine CIP had a flake-like structure with diameters > 5 µm. After effective wet-milling, the native CIP was converted to the uniform nano-sized particles with needle-like shapes. The raw PMB appeared as the fragments of fragile particles. The needle-shaped CIP nanoparticles were transformed into aggregates with a size of approximately 2 µm after spray-drying processes. The spray-dried PMB particles were wrinkled. The F2, F3, and F4 spray-dried particles had irregular shapes.

3.4 Polymorphic forms

The X-ray diffraction pattern of pristine CIP illustrated well-defined and sharp peaks at 2θ of 14.42°, 20.72°, and 25.30° (Figure 2), which was closely matched with the diffractogram of CIP zwitterionic anhydrate form of the Cambridge Crystallographic Data Centre (**Figure S2**). The wet-milled CIP particles exhibited diffraction peaks at 2θ of 6.37°, 23.32°, and 25.83°, indicating that these nanoparticles were in hydrate forms. Among various X-ray diffractogram patterns of CIP

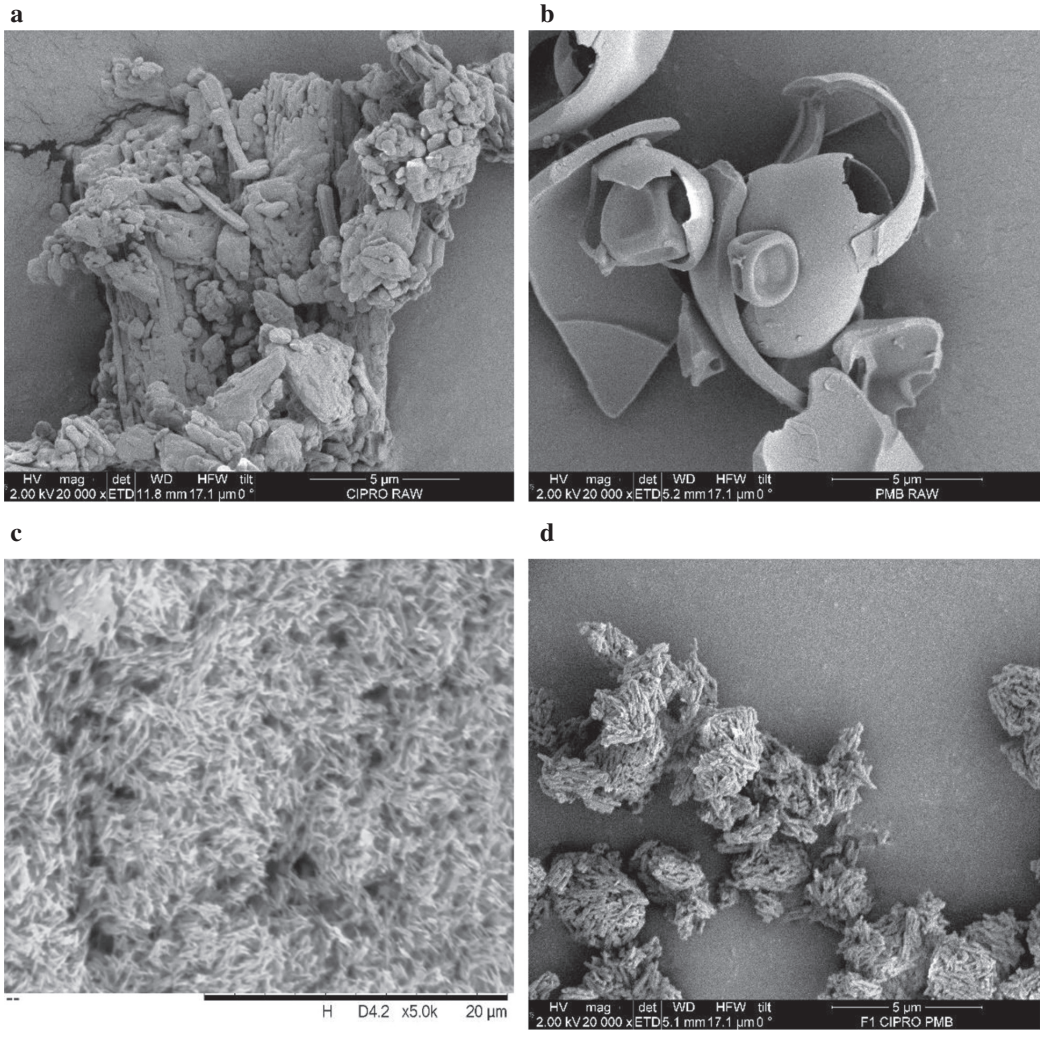

Figure 1 | Continued

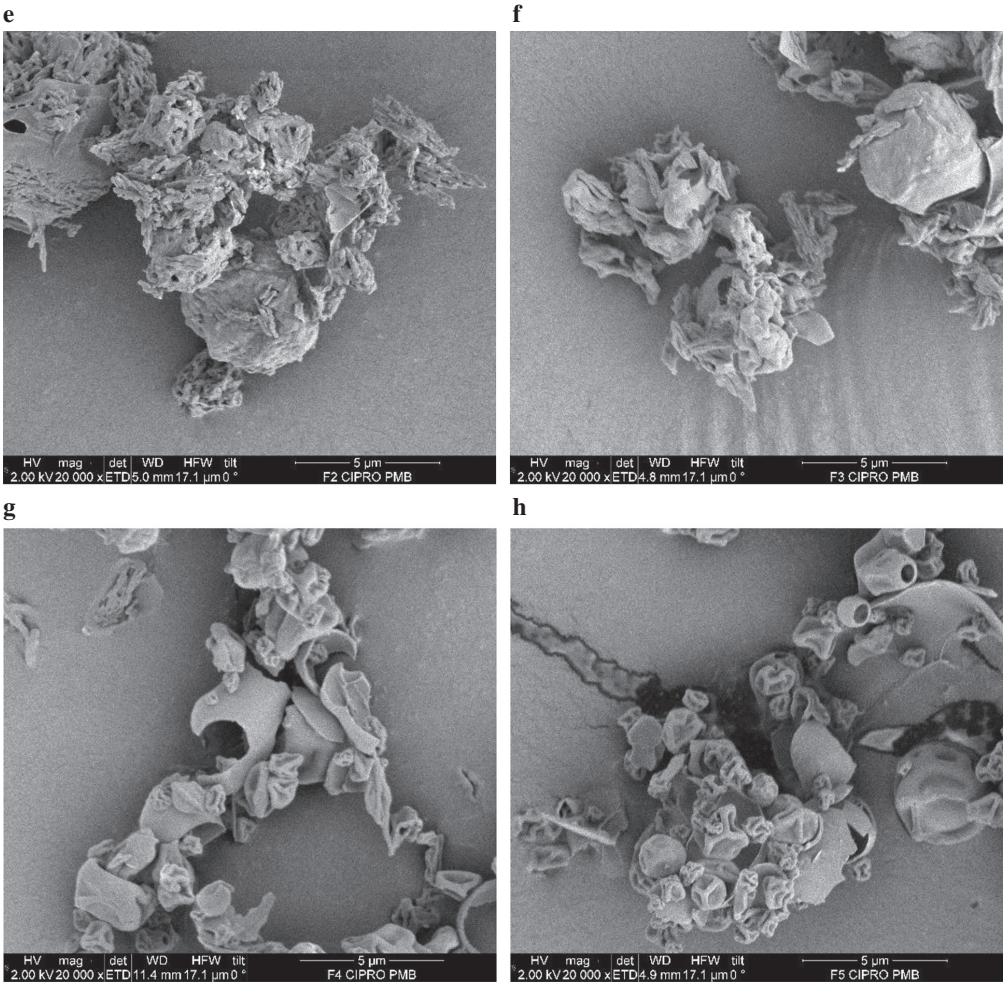

Figure 1 | SEM images of native CIP (a) and PMB (b), wet-milled CIP (c), and spray-dried formulations (F1: d, F2: e, F3: f, F4: g and F5: h).

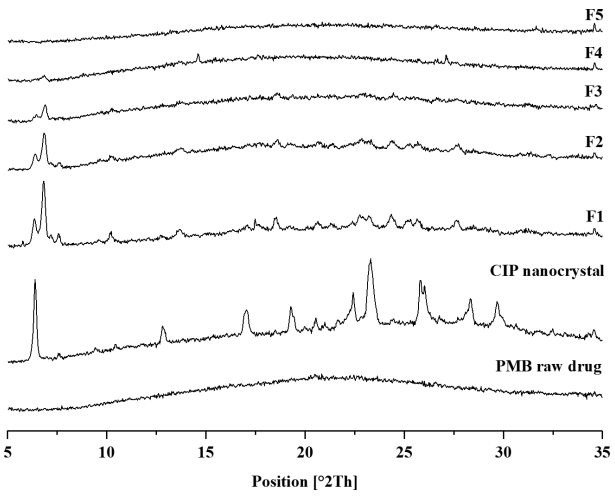

Figure 2 | X-ray diffractograms of PMB raw materials, CIP nanocrystal, and F1-F5.

hydrate forms, hydrate form II (i.e., CIP 4.8 hydrate) was closely matched, and thus hydrate form II was the most probable polymorphic form of the micronized CIP. The attenuated intensity of diffraction peaks and halo pattern of wet-milled CIP implied that CIP was also partly transformed to the amorphous state after processing. Based on the X-ray diffractogram of spray-dried powder F1, the CIP nanoparticle polymorphs were most likely transformed from hydrate form II (i.e., CIP 4.8 hydrate) to hydrate form III (i.e., CIP 3.7 hydrate) in F1 after spray drying. Transformation of polymorphs might be owing to the loss of water molecules during the spray drying process. The X-ray diffractograms of both native PMB and spray-dried powders (F5) confirmed the amorphous nature with no apparent diffraction peaks. When the PMB content was increased in F2-to-F4, the crystallinity of CIP progressively decreased, and interestingly spray-dried powders F4 were nearly in an amorphous state.

Acta Materia Medica

3.5 DSC analyses

The DSC thermogram of native CIP showed an endothermic melting peak at 273 °C. In contrast, the F1 thermal curve displayed two endothermic peaks at 75 °C and 263 °C (Figure 3a). The first peak was ascribed to water evaporation, while the second signal indicated the sample melting phenomenon. The decreased CIP melting point in the spray-dried powder (F1) could be due to reduced crystallinity after the spray-drying process.

Various amorphous samples, including native PMB and spray-dried powders (F1-F5), were subjected to glass transition temperature (T_g) analyses within a wide temperature range (5-200 °C). Because pristine CIP has high crystallinity, CIP was excluded from the T_g analyses. The T_g of raw PMB was 165.06 °C, which was decreased in F5 (148.91 °C). This finding might be credited to the higher water content in F5, which could act as a plasticizer. The presence of spray-dried powders F1 T_g (45.86 °C) could prove that CIP in F1 was partly in amorphous state. The T_g values of various spray-dried powders were enhanced with an increase in the proportions of PMB in the formulations. The samples, such as F2, F3, and F4, displayed a single T_g at 102.03 °C, 104.51 °C, and 112.08 °C, respectively. As reported, the T_g value of CIP varies from 86.7 °C to > 0 °C. The co-spray dried powders (F2, F3, and F4) exhibited the T_g values within the T_g of PMB and CIP. This finding implied the existence of potential interactions between CIP and PMB, and the formation of a drug-drug co-amorphous state within the powders. The potential drug-drug interactions could promote the stability of powders during storage.

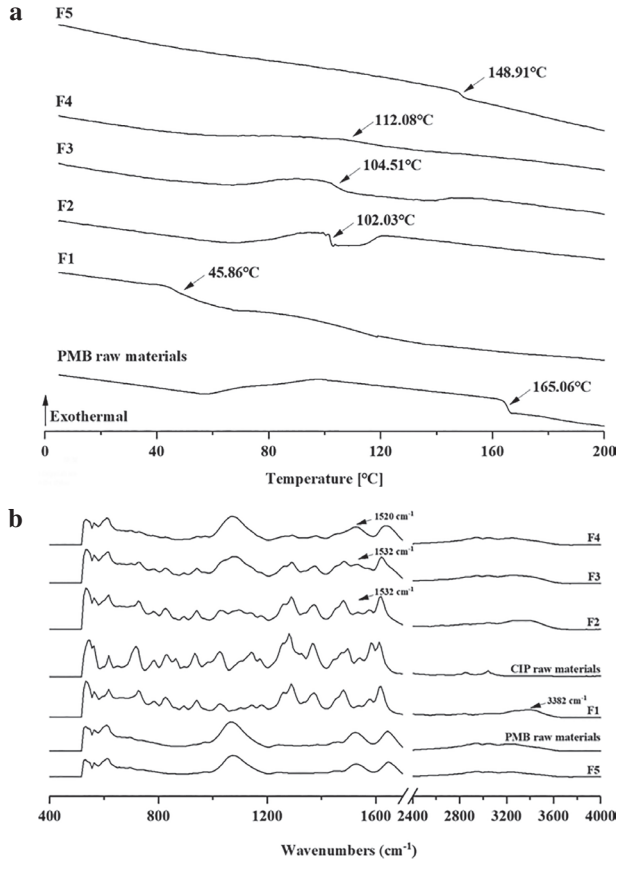

Figure 3 | Representative DSC reversing heat flow thermograms of PMB raw materials and F1-F5 formulations (a), and infrared spectra of F1-F5 formulations, CIP, and PMB raw materials (b).

3.6 FT-IR analyses

To understand potential interactions between CIP and PMB in the spray-dried powders, the FT-IR spectra of native drugs and spray-dried powders were compared (Figure 3b). The FT-IR patterns of raw PMB and spray-dried powders (F5) were analogous without any drifting, indicating no interactions after spray-drying. The FT-IR patterns of raw CIP was quite similar to F1 within the wavenumber region of 400-3200 cm^{-1}, but a new, broad, strong band was observed at 3382 cm^{-1}. This finding was accredited to the N-H or O-H stretching bands, which appeared due to hydrogen bond formation between carboxyl or secondary amine of CIP and water molecules introduced during the formulation process. The IR spectra of F2, F3, and F4 depicted π-π electron-donor-acceptor interactions between CIP and PMB molecules, causing significant shifting of aromatic C = C bonds from 1536 cm^{-1} to a lower wavenumber. Among these formulations, the spray-dried powders F4 demonstrated the most apparent drifted aromatic C = C peak. An equal molar ratio of CIP and PMB (i.e., 1.1:1.0) could interact within spray-dried powders (F4), leading to the strongest interactions and most notable shifted peak.

3.7 Aerodynamic properties

To access the reproducibility in the preparation of various co-spray dried powders, three batches of samples were afforded and the deposited mass content differences of CIP and PMB at each stage in NGI were examined. The lowest reproducibility was observed in F1 and progressively improved as the content of PMB was increased in the powders (Figure 4). For example, > 6 significant differences were evidenced between the CIP mass content and PMB among 3 batches of F2, implying that the drug segregation might be severe, especially in the stage areas (from stage 1 to MOC) when CIP nanosuspensions and PMB solutions were co-spray-dried by a weight ratio of 4:1. The variation in the CIP and PMB mass content was lesser in F3 compared to F2. Significant differences in drug content were only evident in capsule, inhaler, throat, and pre-separator stages among various batches of F3. There were no significant differences in the drug content in stage areas, demonstrating CIP and PMB of F3 might be deposited in the same areas of lungs when the aerodynamic diameters are < 6.12 μm. The differences in drug content was further reduced in

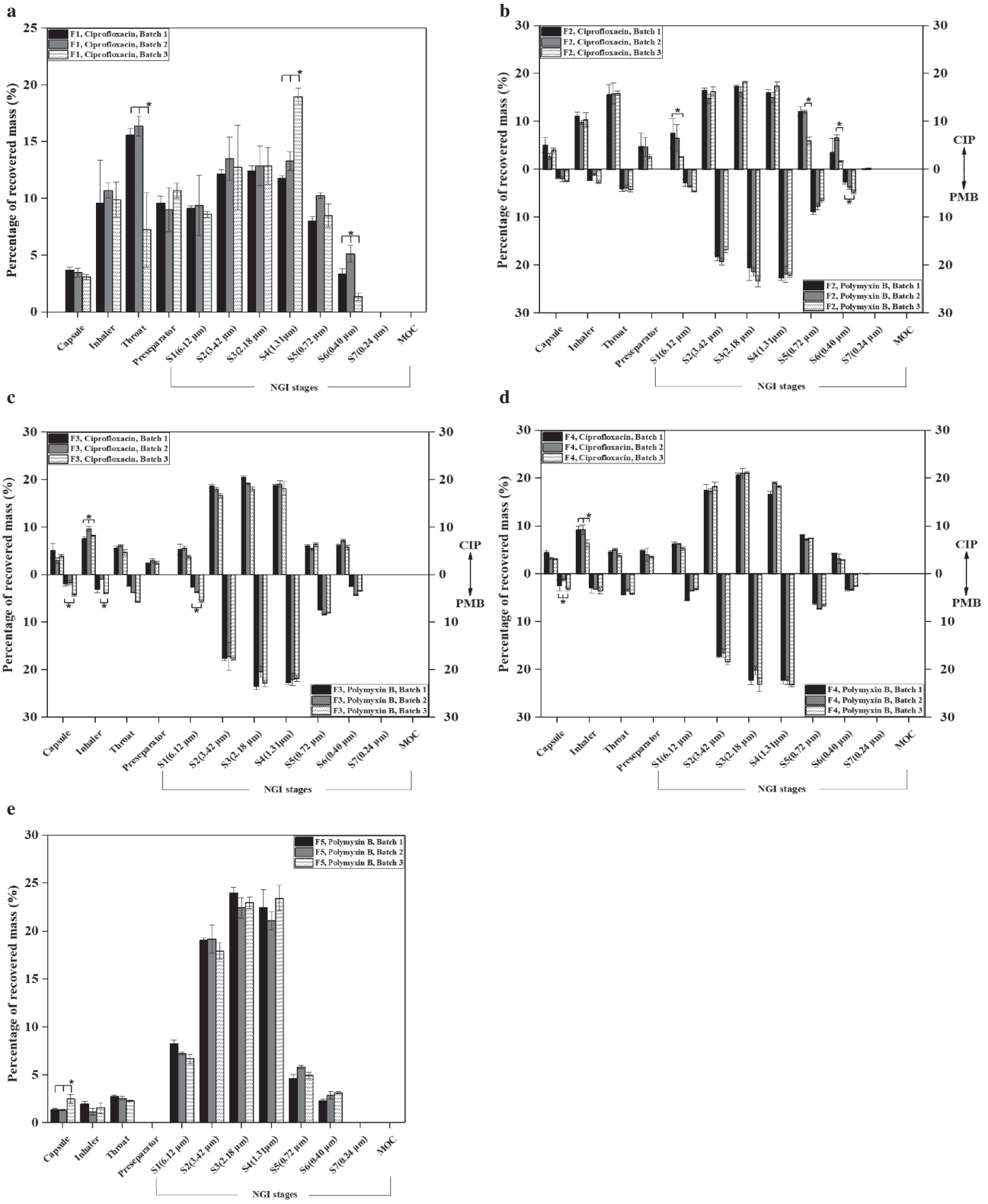

Figure 4 | Aerodynamic assessment of spray-dried formulations from F1-F5 (* = $p < 0.05$) (F1: a, F2: b, F3: c, F4: d and F5: e).

Acta Materia Medica

F4 compared to F2 and F3. Only the inhaler and pre-separator displayed significant differences for drug segregation among three batches of F4, which indicated that CIP and PMB would be deposited in the same areas of the lungs, capsule, and throat parts. F5 had the highest reproducibility and had only one significant difference in drug content at the capsule part.

When the CIP and PMB were co-spray-dried to prepare F2, F3, and F4, the reproducibility among batches was positively correlated with the molar ratios of CIP and PMB used in formulations. The strongest interaction forces between CIP and PMB existed in F4, leading to the lowest variability in mass content of drugs because CIP and PMB could be distributed more evenly in spray-dried powders. The restricted interactions in F2 might interfere with the integration between CIP and PMB and cause the content segregation. As the concentration of poorly-soluble CIP was higher in F2 (16 mg/mL) than F4 (4 mg/mL), the particle size of CIP in F2 was more likely to be bigger than the particle size of CIP in F4. According to Stoke's law, the larger particles of F2 sediment faster and resulted in extraordinarily obvious drug segregation relative to F4.

Various parameters, such as FPF_{total} (%), ED (%), RD (mg), and MMAD (μm), were estimated to compare the aerodynamic properties among three batches of spray-dried powders (F1-F5; **Table 3**). The ED (%) refers to the total recovered drug mass from the throat, pre – separator, all stages, and MOC with respect to the mass of drug loaded in the capsule. The RD is the drug mass from the throat, pre-separator, all stages, and MOC. The FPF_{total} (%) is defined as the mass of drug with an aerodynamic diameter < 5.0 μm with respect to the mass of drug loaded in the capsule. The MMAD reflects the diameters of 50% of particles (based on the mass), which are above and below of the aerodynamic diameters. Interestingly, no significant difference was revealed for each drug among three batches in a specific formulation. The FPF_{total} (%) values of PMB were much higher compared to CIP, which might be ascribed to the surface morphology of the drug particles. The wet-milled, needle-shaped CIP nanocrystals were agglomerated following the spray-drying process. In contrast, PMB molecules tended to form porous and round-shaped particles upon spray drying. Thus, the needle-like CIP particles had a lower flowability than the porous, round particles of PMB. The CIP particles also induced high Van der Waals forces and cohesive attractions among themselves and resulted in poorer dispersibility, which would lead to lower values of FPF_{total} (%). A dramatically improved FPF_{total} (%) value of CIP was observed in F2, F3, and F4 than F1 ($p < 0.05$), confirming that PMB improved the aerodynamic performance of CIP after being co-spray dried. The improved aerodynamic performance of CIP might be accredited to the enriched surface concentration of PMB. The PMB molecules could be self-assembled into porous round particles and the CIP nanocrystals were sheltered in those particles after spray drying, which were also revealed in their SEM images.

To further investigate the influences of different powder doses on the aerodynamic properties, variable amounts (10, 20, and 30 mg) of spray-dried powder of each formulation were sealed in the capsules, tested for the aerodynamic behavior, and compared (**Figure 5**).

It was noticed that the mass fractions of inhalable dry powders became lower when the masses of loaded drug were increased from 10-to-20 mg and higher, which might also reduce the FPF_{total} (%) values (**Figure 6**). It suggested that the aerodynamic performance would be enhanced when a loaded drug mass was 10 mg compared to 20 mg and 30 mg. This problem might be caused by the limited dispersibility of the dry powders and confined aerosolization ability of inhaler and pump. Moreover, as the FPF_{total} (%) values for 20 mg and 30 mg loaded drug mass were significantly reduced, these might cause more drug waste during inhalation.

Table 3 | FPF_{total}, ED, RD, and MMAD values of various spray-dried powders.

Formulation	Drug	FPF_{total} (%)			ED (%)			RD (mg)			MMAD (μm)
		Batch 1	Batch 2	Batch 3	Batch 1	Batch 2	Batch 3	Batch 1	Batch 2	Batch 3	
F1	CIP	55.5 ± 2.2	54.0 ± 2.3	55.9 ± 1.4	79.2 ± 0.4	78.4 ± 0.5	79.8 ± 0.4	9.1 ± 0.3	9.4 ± 0.0	8.9 ± 0.0	2.41 ± 0.09
F2	CIP	62.4 ± 3.1	63.7 ± 2.4	62.4 ± 0.0	79.7 ± 1.1	80.9 ± 2.1	78.7 ± 1.7	6.5 ± 0.0	7.3 ± 0.1	6.8 ± 0.1	2.35 ± 0.13
	PMB	75.2 ± 5.3	76.2 ± 3.9	71.1 ± 1.2	84.3 ± 6.4	84.9 ± 5.9	82.4 ± 3.6	2.0 ± 0.1	2.2 ± 0.1	2.2 ± 0.0	
F3	CIP	64.5 ± 0.1	64.8 ± 1.3	64.5 ± 0.1	81.4 ± 2.1	82.7 ± 0.5	79.0 ± 0.0	5.1 ± 0.1	4.7 ± 0.0	3.9 ± 0.0	2.33 ± 0.21
	PMB	77.7 ± 0.5	77.8 ± 0.9	78.2 ± 1.5	84.7 ± 4.2	85.4 ± 1.5	87.4 ± 1.6	5.9 ± 0.3	5.4 ± 0.1	4.3 ± 0.1	
F4	CIP	65.6 ± 0.6	65.7 ± 1.2	65.1 ± 0.5	80.5 ± 1.0	81.6 ± 2.2	77.6 ± 2.2	2.0 ± 0.0	1.8 ± 0.0	1.5 ± 0.0	2.28 ± 0.07
	PMB	73.0 ± 0.8	71.6 ± 1.1	74.7 ± 0.7	80.5 ± 3.7	80.4 ± 3.5	84.2 ± 1.9	9.7 ± 0.3	8.9 ± 0.3	7.2 ± 0.1	
F5	PMB	75.3 ± 1.3	74.6 ± 0.9	73.8 ± 1.1	87.3 ± 0.6	87.1 ± 0.8	86.1 ± 0.9	10.6 ± 0.0	10.6 ± 0.1	9.4 ± 0.1	2.24 ± 0.03

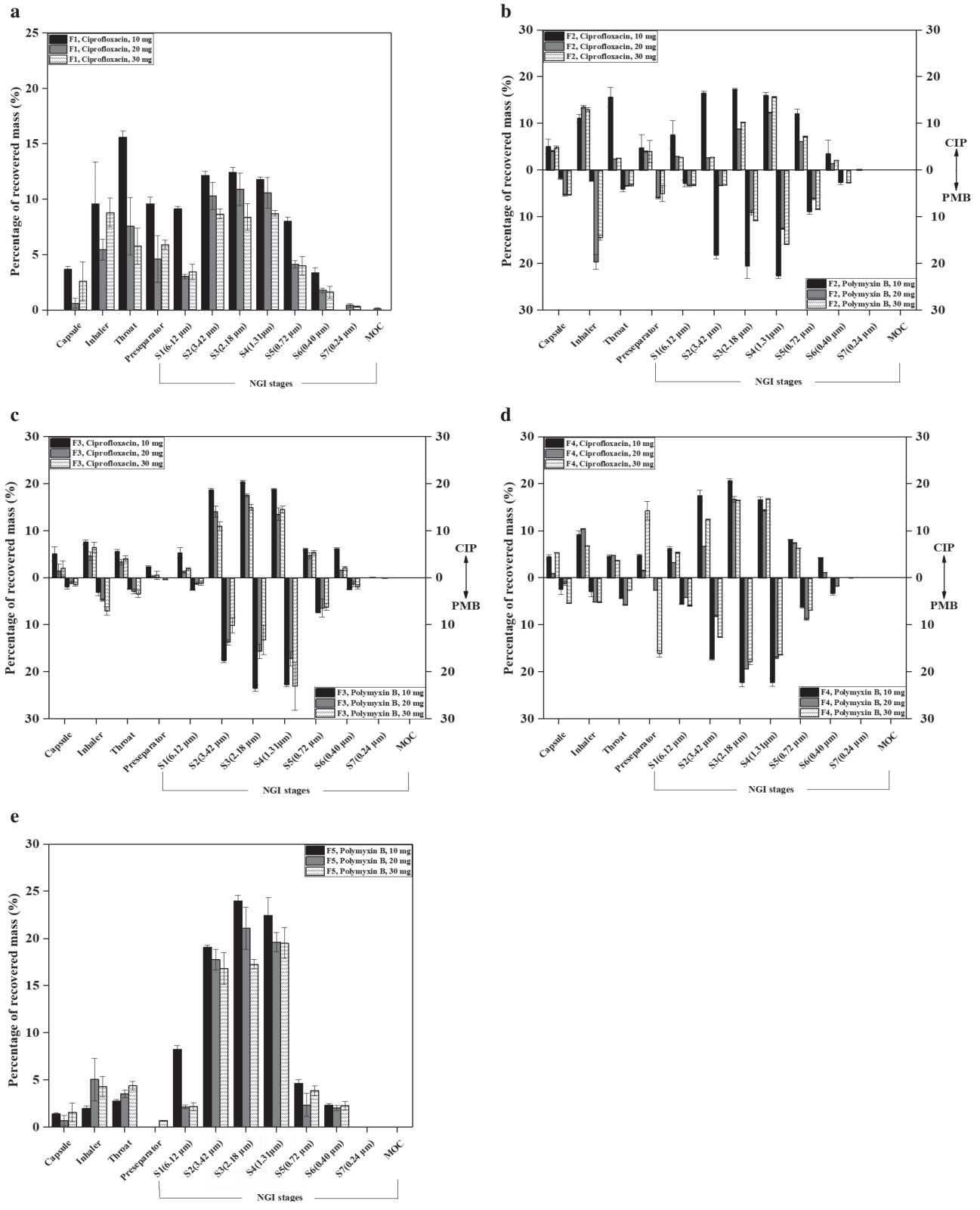

Figure 5 | Aerodynamic assessment of spray-dried formulations from F1-F5 with different powder doses (10, 20, and 30 mg sealed in the capsules; F1: a, F2: b, F3: c, F4: d and F5: e).

Acta Materia Medica

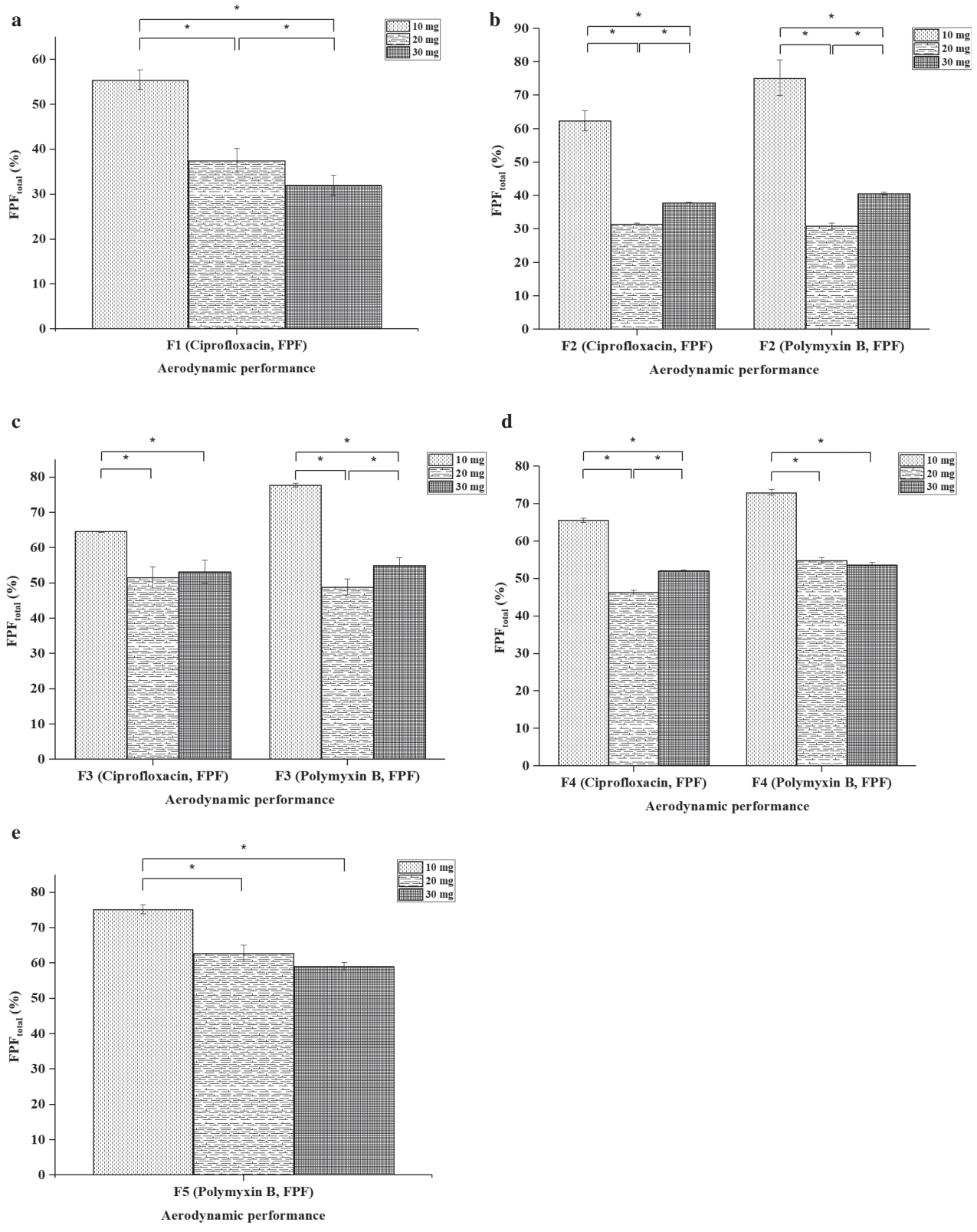

Figure 6 | FPF$_{total}$ (%) values of spray-dried formulations from F1-F5 with different powder doses (10, 20, and 30 mg sealed in the capsules; F1: a, F2: b, F3: c, F4: d and F5: e).

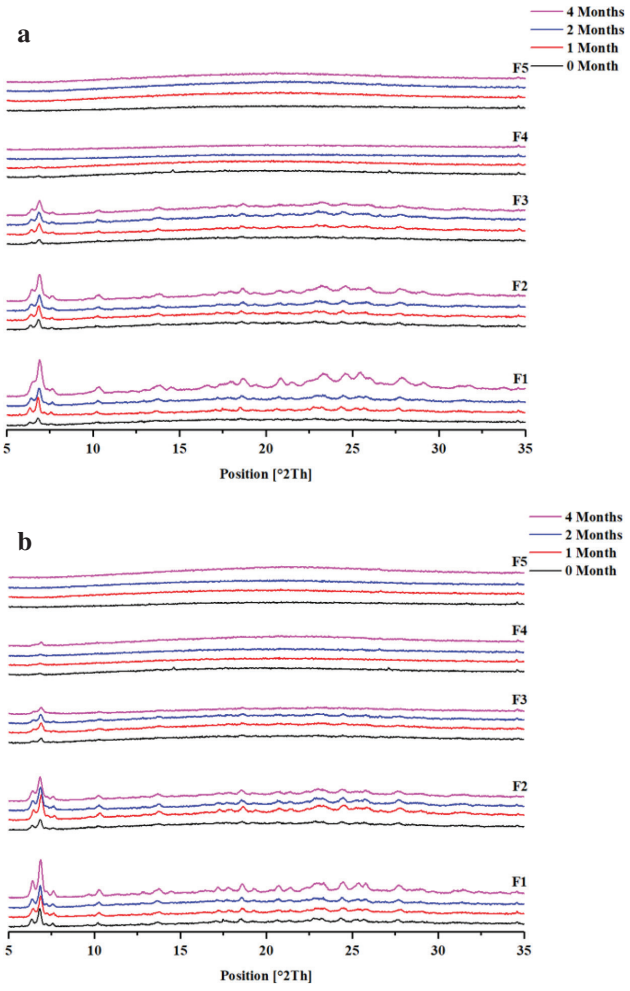

Figure 7 | X-ray diffractograms of F1-F5 formulations from 0-4 months under 60% RH and room temperature (a), and 3% RH and room temperature (b).

3.8 Antibacterial susceptibility test

Different formulations with a drug mass concentration of 250 μg/mL, which was much higher than the PAO1 minimal inhibitory concentrations [MICs] (CIP, 0.06 μg/mL; and PMB, 0.5 μg/mL), was transferred to Muller-Hinton agar plates inoculated with PAO1. All these spray-dried formulations established the inhibition ability to PAO1 by showing inhibition zones, which varied among F1-F5. PAO1 represented the highest susceptibility to F1 with an inhibition zone size of 16 mm (Table 2). The inhibition ability of the formulations to PAO1 was decreased as the PMB content was increased. Consequently, F5 demonstrated the lowest inhibition ability to PAO1 with zone size of 10 mm (Table 2). The results indicated that the PAO1 was more susceptible to CIP than PMB and CIP was more effective in killing planktonic cells. Therefore, the inhibition ability of PMB to PAO1 could be improved by adding CIP with fixed total drug mass as the inhibition zone sizes of F2, F3, and F4 were > F5.

3.9 Stability studies

The potential influences of storage conditions on the drug crystallinity and aerodynamic properties of the spray-dried powders were characterized (Figure 7 and Table 4). There was no apparent change depicted in the X-ray diffractograms of F1-F5 under both storage conditions (Figure 7); however, a slight increase in the CIP crystallinity was observed after 4 months under both storage conditions as the peak at 2θ of 6.37° of CIP was intensified.

The FPF_{total} (%) values of various formulations (F1-F5) stored for 1-4 months under 2 different conditions were calculated to assess the aerodynamic properties (Table 4). When spray-dried powders were stored < 60% RH and room temperature for 4 months, there were no significant changes in the FPF_{total} (%) of PMB for F4. The significant decrease in the FPF_{total} (%) value of PMB

Table 4 | FPF_{total} (%) values of various formulations measured during stability testing.

Formulation Code	Drug	60% Relative Humidity, Room Temperature				3% Relative Humidity, Room Temperature			
		FPF_{total} (%)				FPF_{total} (%)			
		0 month	1 month	2 months	4 months	0 month	1 month	2 months	4 months
F1	CIP	55.5 ± 2.2	52.8 ± 6.0	57.7 ± 3.5	49.6 ± 1.5	55.5 ± 2.2	54.6 ± 1.3	54.5 ± 3.9	53.9 ± 2.9
F2	CIP	62.4 ± 3.1	69.3 ± 4.9	65.3 ± 2.5	72.3 ± 5.4	62.4 ± 3.1	60.4 ± 1.5	61.9 ± 2.4	63.9 ± 1.1
	PMB	75.2 ± 5.3	66.9 ± 3.0	73.4 ± 3.2	81.0 ± 2.0	75.2 ± 5.3	73.4 ± 0.7	73.2 ± 2.2	72.5 ± 5.1
F3	CIP	64.5 ± 0.1	70.5 ± 0.8	74.8 ± 0.5	70.9 ± 7.9	64.5 ± 0.1	62.6 ± 0.7	66.2 ± 1.2	67.8 ± 0.3
	PMB	77.7 ± 0.5	68.0 ± 1.7	71.6 ± 1.1	70.2 ± 6.8	77.7 ± 0.5	70.5 ± 0.5	72.8 ± 0.9	73.7 ± 0.5
F4	CIP	65.6 ± 0.6	62.5 ± 3.0	72.3 ± 2.0	78.2 ± 6.3	65.6 ± 0.6	61.1 ± 1.6	62.6 ± 1.6	66.7 ± 1.6
	PMB	73.0 ± 0.8	67.2 ± 3.7	74.0 ± 2.4	77.4 ± 6.5	73.0 ± 0.8	71.2 ± 1.3	73.7 ± 2.4	74.0 ± 2.0
F5	PMB	75.3 ± 1.3	69.3 ± 0.7	71.5 ± 1.2	79.2 ± 4.2	75.3 ± 1.3	73.5 ± 1.4	72.7 ± 1.9	75.3 ± 3.8

in F3 might be due to agglomeration and caking ($p < 0.05$). While the FPF_{total} (%) for CIP in F1, F2, F3, and F4 were significantly increased ($p < 0.05$) after 4 months of storage. The increase in the FPF_{total} (%) for CIP after 4 months of storage was ascribed to the recrystallization of CIP molecules, which could increase the surface roughness and reduce the interactions between particles, improving aerodynamic properties. After 4 months of storage, the CIP in F2 exhibited a greater deposition at stages 2 and 4. For CIP in F3 and F4, a superior deposition was observed at stages 3 and 4. The increased depositions at these stages might improve aerodynamic properties.

When various spray-dried powders (F1-F5) were stored under 3% RH and room temperature, no significant change was observed in the FPF_{total} (%) values, even after 4 months. This finding signified that the condition of 3% RH and room temperature would be a more suitable for storage for these spray-dried powders than the condition of 60% RH and room temperature.

4. CONCLUSIONS

In the present study the CIP nanosuspensions were co-spray-dried with PMB solutions to accomplish inhalable CIP/PMB dry powders, which demonstrated promising aerodynamic properties. The formulations exhibited high and reproducible FPF total (%) values, which enabled the formulations to be effectively deposited in the pulmonary tract. Indeed, π-π electron-donor-acceptor interactions might exist between CIP and PMB in the co-spray-dried formulations. The co-amorphous state might also assist the spray-dried powders to achieve stable physical properties under a storage condition of 3% relative humidity and room temperature for 4 months. The formulations illustrated excellent antimicrobial ability against PAO1. According to the experimental results, it was understood that the formulations containing more PMB might improve the aerodynamic performances and stability. On the other hands, a higher PMB content in the formulation might decrease the inhibition potential against PAO1. Thus, further characterization of these inhalable dry powders in a suitable *in vivo* model might guide us to select a best formulation. Thus, the inhalable dry powders of CIP and PMB could be a promising combination therapy against respiratory infections.

REFERENCES

[1] Armstrong DS, Grimwood K, Carzino R, Carlin JB, Olinsky A, Phelan PD: Lower respiratory infection and inflammation in infants with newly diagnosed cystic fibrosis. *British Medical Journal* 1995, 310:1571–1572.

[2] Miravitlles M, Anzueto A: Chronic respiratory infection in patients with chronic obstructive pulmonary disease: what is the role of antibiotics? *International Journal of Molecular Sciences* 2017, 18:1344.

[3] Troeger C, Blacker B, Khalil IA, Rao PC, Cao J, Zimsen SR, et al.: Estimates of the global, regional, and national morbidity, mortality, and aetiologies of lower respiratory infections in 195 countries, 1990–2016: a systematic analysis for the Global Burden of Disease Study 2016. *The Lancet Infectious Diseases* 2018, 18:1191–1210.

[4] Goossens H, Ferech M, Vander Stichele R, Elseviers M: ESAC Project Group: Outpatient antibiotic use in Europe and association with resistance: a cross-national database study. *The Lancet.* 2005, 365:579–587.

[5] Zhou QT, Leung SS, Tang P, Parumasivam T, Loh ZH, Chan HK: Inhaled formulations and pulmonary drug delivery systems for respiratory infections. *Advanced Drug Delivery Reviews* 2015, 85:83–99.

[6] Herrmann G, Yang L, Wu H, Song Z, Wang H, Høiby N, et al.: Colistin-tobramycin combinations are superior to monotherapy concerning the killing of biofilm Pseudomonas aeruginosa. *The Journal of Infectious Diseases* 2010, 202:1585–1592.

[7] Shetty N, Ahn P, Park H, Bhujbal S, Zemlyanov D, Cavallaro A, et al.: Improved physical stability and aerosolization of inhalable amorphous CIP powder formulations by incorporating synergistic colistin. *Molecular Pharmaceutics* 2018, 15:4004–4020.

[8] Ye T, Sun S, Sugianto TD, Tang P, Parumasivam T, Chang YK, et al.: Novel combination proliposomes containing tobramycin and clarithromycin effective against Pseudomonas aeruginosa biofilms. *International Journal of Pharmaceutics.* 2018, 552:130–138.

[9] Wang S, Yu S, Lin Y, Zou P, Chai G, Heidi HY, et al.: Co-delivery of ciprofloxacin and colistin in liposomal formulations with enhanced in vitro antimicrobial activities against multidrug resistant Pseudomonas aeruginosa. *Pharmaceutical Research.* 2018, 35:1–3.

[10] Yu S, Wang S, Zou P, Chai G, Lin YW, Velkov T, et al.: Inhalable liposomal powder formulations for co-delivery of synergistic ciprofloxacin and colistin against multi-drug resistant gram-negative lung infections. *International Journal of Pharmaceutics.* 2020, 575:118915.

[11] Chow AH, Tong HH, Chattopadhyay P, Shekunov BY. Particle engineering for pulmonary drug delivery. *Pharmaceutical Research.* 2007, 24:411–437.

[12] Holloway AB, Morgan AF. Genome organization in Pseudomonas. *Annual Reviews in Microbiology* 1986, 40:79–105.

[13] Wang J, Stegger M, Moodley A, Yang M. Drug combination of ciprofloxacin and polymyxin b for the treatment of multidrug–resistant acinetobacter baumannii infections: a drug pair limiting the development of resistance. *Pharmaceutics* 2023, 15:720.

[14] Yang JZ, Young AL, Chiang PC, Thurston A, Pretzer DK. Fluticasone and budesonide nanosuspension for pulmonary delivery: preparation, characterization, and pharmacokinetic studies. *Journal of Pharmaceutical Sciences* 2008, 97:4869–4878.

[15] Liu T, Han M, Tian F, Cun D, Rantanen J, Yang M. Budesonide nanocrystal-loaded hyaluronic acid microparticles for inhalation: In vitro and in vivo evaluation. *Carbohydrate Polymers* 2018, 181:1143–1152.

[16] Hudzicki J. Kirby-Bauer disk diffusion susceptibility test protocol. *American Society for Microbiology* 2009, 15:55–63.

[17] Manual D. Dehydrated culture media and reagents for microbiology. Laboratories incorporated Detroit. *Michigan* 1984, 48232:1027.
[18] Høiby N, Henneberg KÅ, Wang H, Stavnsbjerg C, Bjarnsholt T, Ciofu O, et al.: Formation of Pseudomonas aeruginosa inhibition zone during tobramycin disk diffusion is due to transition from planktonic to biofilm mode of growth. *International Journal of Antimicrobial Agents*. 2019, 53:564–573.